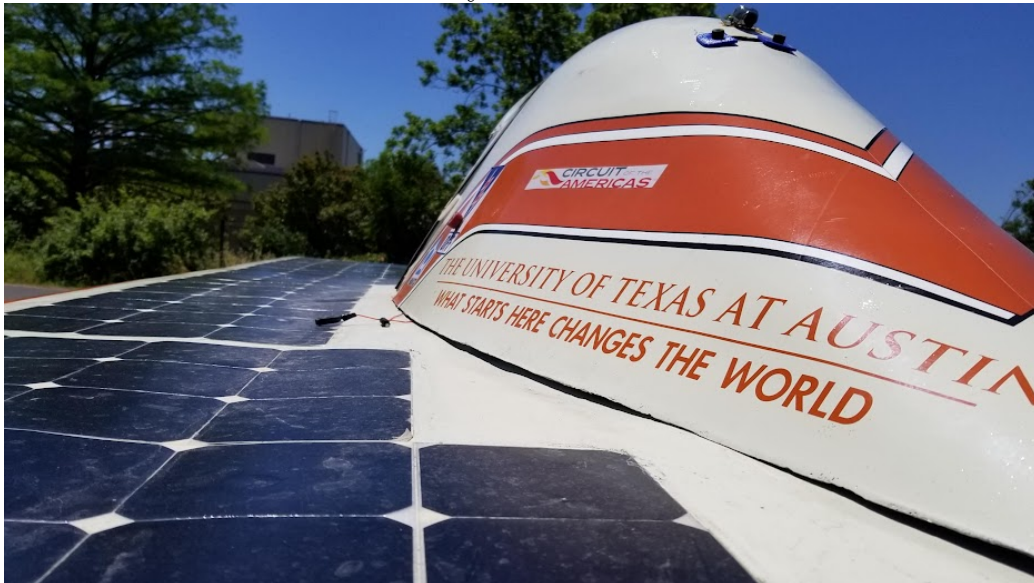


# Evaluation and Improvement of Photovoltaic Power Systems

The University of Texas at Austin



Matthew Junkit Yu

17 December 2022

# Contents

<b>1</b>	<b>Introduction</b>	<b>5</b>
<b>2</b>	<b>Modeling Photovoltaics</b>	<b>8</b>
2.1	Three Parameter Solar Cell Model . . . . .	9
2.1.1	Model Introduction . . . . .	9
2.1.2	Photocurrent . . . . .	10
2.1.3	Dark Current . . . . .	11
2.1.4	Dark Saturation Current . . . . .	12
2.1.5	Short Circuit Current . . . . .	13
2.1.6	Open Circuit Voltage . . . . .	15
2.1.7	Model Summary . . . . .	17
2.2	Five Parameter Solar Cell Model . . . . .	19
2.2.1	Model Introduction . . . . .	19
2.2.2	Shunt Resistance . . . . .	19
2.2.3	Series Resistance . . . . .	20
2.3	Seven Parameter Solar Cell Model . . . . .	21
2.4	Evaluation of Solar Cell Models . . . . .	22
2.4.1	Solar Cell Dataset . . . . .	22
2.4.2	Methods to Fit Cells . . . . .	22
2.5	Modeling Solar Modules . . . . .	23
2.6	Evaluation of Solar Module Models . . . . .	24
2.7	Modeling Solar Arrays . . . . .	25
2.8	Evaluation of Solar Array Models . . . . .	26
<b>3</b>	<b>Optimizing Photovoltaics</b>	<b>27</b>
<b>4</b>	<b>Optimizing Photovoltaic Systems</b>	<b>28</b>

<b>5 Conclusion</b>	<b>29</b>
<b>Appendices</b>	<b>32</b>
<b>A Acronyms and Abbreviations</b>	<b>33</b>
<b>B Mathematical Nomenclature</b>	<b>34</b>

# List of Figures

2.1	Three Parameter, or Single Diode Model of a Solar Cell . . . .	9
2.2	Maxeon Gen III Cell Spectral Response . . . . .	11
2.3	Solar Cell Temperature Dependence . . . . .	14
2.4	Solar Cell Irradiance Dependence . . . . .	15
2.5	Five Parameter, or Full Single Diode Model of a Solar Cell . .	19
2.6	Effect of Series (a) and Shunt Resistance (b) on current-voltage (I-V) Curve . . . . .	20
2.7	Seven Parameter, or Double Diode Model of a Solar Cell . . .	21

# List of Tables

2.1	Various Ideality Factors of ideality factor $(n)$ . . . . .	12
-----	---	----

# Chapter 1

## Introduction

In order to reach net zero emissions targets set by the United Nations (UN) at the 2015 Paris Agreement [13] before 2050, the International Energy Association (IEA) estimates that nearly 630 Gigawatts (GW) [11] of photovoltaic (PV) energy generation capacity need to be added annually by 2030. As of 2022, we observed that at least 175 GW were installed in 2021 [9] [8], a 22% year over year growth. With large policy and geopolitical tailwinds behind major economies like the United States and Europe, solar is expected to be one of the, if not the major driver of new energy generation within the next two decades.

However, in order to achieve this target generation capacity in a sustainable way, engineers and PV designers need to maximize the electrical efficiency of the overall power system, as opposed to just improving the solar cell efficiency. According to the U.S. Energy Information Administration (EIA) [15], the capacity factor of PVs as an energy source in the United States reached a monthly maximum of 33.4% in June of 2022; *capacity factor* is defined by the EIA as a measure of the generated output by the electric generator versus the maximum possible output. It is clear that system inefficiencies in PV generation provide large constraints, and optimistically, equally large opportunities, in allowing us to increase our pace towards reaching net zero carbon emissions by 2050.

This thesis takes a holistic evaluation of the PV power generation system in a unique use case that necessitates maximizing the capacity factor: solar powered vehicles. We evaluate the modeling, creation, and optimization of a solar powered vehicle for the University of Texas at Austin’s Longhorn Racing Solar (LHRs) team, and attempt to identify and address inefficiencies and

bottlenecks whose improvements will help the larger **PV** industry as a whole.

In particular, this thesis will focus on three important and active areas of development within the **PV** field: solar array modeling and prediction, solar cell binning processes and heuristics, and maximum power point tracking (**MPPT**) algorithms. In each of these areas, we look at the state of the art techniques, propose novel ideas to improve our understanding of the system and its inefficiencies, and see if we can translate it lateral applications like rooftop solar or industrial **PV**. Note that in this thesis we refer to photovoltaics and solar without distinction.

In the first major chapter, **Modeling Photovoltaics**, this thesis discusses how can solar cells can be modeled at various abstraction layers, from idealized cells at standard conditions using the 3-parameter model to non-idealized cells that incorporate parasitic resistances using the 7-parameter model. These solar cell models are then evaluated against a dataset of several hundred solar cell **I-V** and power-voltage (**P-V**) curves generated from our custom testing setup to see how well the model fits real cells at different conditions. We build upon these models to form larger units of **PVs**, such as solar modules and solar arrays, which may consist of strings of cells in series with bypass diodes across them, among other configurations. Some important topics that are explored using these multi-cell models include **PV** mismatch and bypass activation. Insights from these topics lead to heuristics that are proposed in the next chapter, **Optimizing Photovoltaics**.

The second major chapter, **Optimizing Photovoltaics**, takes the aforementioned models and dataset created to propose a process to bin, match, and combine solar cells and modules, with the end goal of maximizing the performance of the solar array that will be attached to the solar vehicle. In this chapter, we propose design criteria, heuristics, and methodologies to generate designs for the solar vehicle that fit the unique constraints of the application, which center around the dynamism of the system as it moves in transit across the real world.

In the third and final major chapter, **Optimizing Photovoltaic Systems**, this thesis investigates the operation of the **PV** system in the context of the solar vehicle. We observe the energy conversion process from incident light on the solar array to electricity captured by the battery protection system (**BPS**) and present a **PV** system simulator and a suite of **MPPT** algorithms to minimize energy losses from the aforementioned conversion process. We demonstrate custom hardware developed by the **LHRs** team and evaluate in real world settings a select set of **MPPT** algorithms. We compare

The second area of development may be more generalized then this.

these results with existing research and our digital twin model of the solar vehicle, and finally discuss conclusions from the three chapters that can be translatable to the wider **PV** industry.

Along with these three major chapter, we also provide a large set of appendices corresponding to the development of the main body of work in this thesis. Among them include manufacturing procedures for testing, assembling, and laminating solar cells into solar modules, schematics and accompanying documentation for hardware that was used for characterizing and validating parts of the thesis, software diagrams with relevant open source software repositories developed by our team, and extra insights into the design of the **LHRs**' photovoltaic array that are not directly applicable to the major chapters, such as thermal models performed of the vehicle topshell that influenced our simulation models, among others.



# Chapter 2

## Modeling Photovoltaics

Insert intro paragraph on the focus of this chapter, as well as the a short discussion of the following sections.

## 2.1 Three Parameter Solar Cell Model

### 2.1.1 Model Introduction

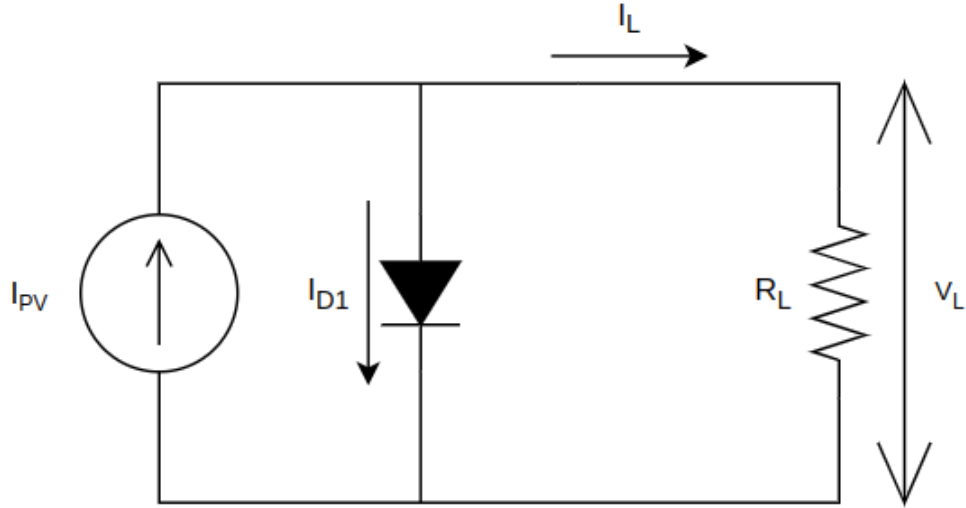


Figure 2.1: Three Parameter, or Single Diode Model of a Solar Cell

The most basic model of a solar cell is the three parameter model, or single diode model, shown in Figure 2.1. It consists of a constant current source and a diode. The constant current source produces a photocurrent, or light generated current ( $I_{PV}$ ) caused by photons of sufficient energy being absorbed into the surface of the solar cell and exciting charge carriers (generally in the form of electrons) to enter the circuit. The diode represents the various recombination processes that consume the generated current in the form of dark current, or diode current ( $I_D$ ).

In this model, the three parameters consist of the following:

- the photocurrent  $I_{PV}$ ,
- a dark saturation current, or reverse saturation current ( $I_0$ ),
- and an  $n$ .

The latter two are contained within the dark current  $I_D$ , and generally influence the shape of the predicted  $I$ - $V$  curve, particularly around the knee-bend.

This model is juxtaposed from the five parameter model in that it does not incorporate cell losses in the form of series resistance ( $R_S$ ) and shunt resistance ( $R_{SH}$ ). It is assumed that the series resistance is zero (short circuit) and the shunt resistance is infinite (open circuit). The five parameter model may also be called the complete single diode model.

We observe from Figure 2.1 that the load current ( $I_L$ ) can be represented as a function of the photocurrent  $I_{PV}$  and the dark current  $I_D$ , shown in Equation 2.1.

$$I_L = I_{PV} - I_D \quad (\text{A}) \quad (2.1)$$

In the following subsections, we break down each component into its constituent parts.

### 2.1.2 Photocurrent

$$I_{PV} = qA \int b_s(E)QE(E)dE \quad (\text{A}) \quad (2.2)$$

On a fundamental level, we can define the photocurrent  $I_{PV}$  as a function of the photons incident upon the surface of the solar cell and the solar cell's spectral response. This is demonstrated in Equation 2.2. A bulleted explanation of this equation oriented for the layman is as follows:

- Incident light hits the solar cell over a given spectrum of energy levels (denoted either in  $eV$  or in  $nm$ ) (see Figure 2.2).
- Incident light at each discrete energy level has an spectral photon flux density ( $b_s(E)$ ), otherwise known as intensity.
- The solar cell has a given quantum efficiency ( $QE(E)$ ) at each energy level, which is the probability that an incident photon of energy ( $E$ ) delivers one electron to the external circuit.
- Integrating the product of the photon flux density  $b_s(E)$  and quantum efficiency  $QE(E)$  (then multiplied by the electric charge constant ( $q$ ) and the cell area ( $A$ )) provides the photocurrent  $I_{PV}$ .

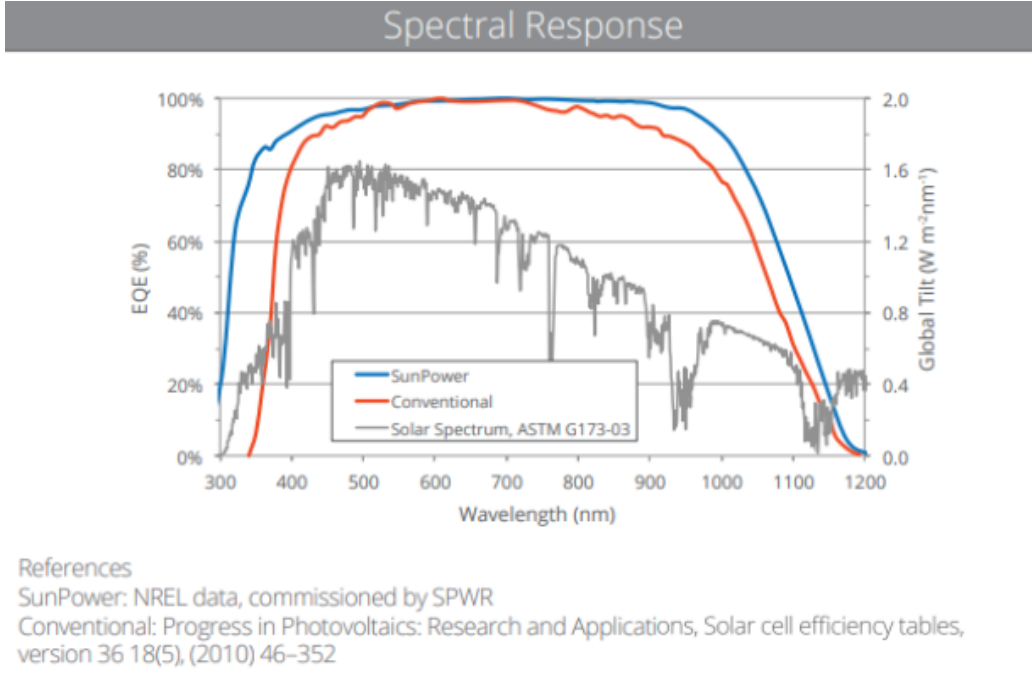


Figure 2.2: Maxeon Gen III Cell Spectral Response

Solar cell manufacturers may provide a spectral response chart showing the quantum efficiency over the useful solar spectrum (as seen in Figure 2.2), but will generally just provide the short circuit current ( $I_{SC}$ ) at standard test conditions (STC) ( $1000 \text{ W m}^{-2}$ ,  $AM\ 1.5G$ ,  $25\text{ }^\circ\text{C}$ ).

As it turns out, the photocurrent  $I_{PV}$  can generally be approximated as the short circuit current  $I_{SC}$ .

$$I_{PV} = I_{SC} \quad (\text{A}) \quad (2.3)$$

We'll discuss in Section 2.2 that Cubas et al. [12] defines the photocurrent as a ratio of the series and shunt resistance in addition to the short circuit current. However, in most cases, the empirical value of  $I_{SC}$  will not differ from Equation 2.3.

### 2.1.3 Dark Current

The dark current  $I_D$  comprises of the interesting and critical parameters of the three parameter model; shown in Equation 2.4, it consists of the term  $I_0$

and an exponential. The exponential is a function of three key variables: the cell temperature ( $T_C$ ), load voltage ( $V$ ), and ideality factor  $n$ .

This ideality factor is typically between 1 and 2, and represents the proportional influence of carriers in several recombination processes for a given cell composition and structure. Some ideality factor values are presented in Table 2.1, sourced from PVEducation’s Ideality Factor page [5]. We note that the ideality factor may be outside the typical range of  $[1, 2]$ , as discussed by Jain et Kapoor [6] and R.N. Hall [3], the latter of which notes that Auger recombination dominated dark currents generate a  $n$  of  $2/3$ .

The term thermal voltage ( $V_T$ ) which encapsulates the  $T_C$  dependency describes the voltage across the P-N junction of the diode in the model: at STC this is typically  $26\text{ mV}$ . It is defined by Equation 2.5.

$$I_D = I_0[\exp(\frac{V}{V_T}) - 1] \quad (\text{A}) \quad (2.4)$$

$$V_T = \frac{nk_B T_C}{q} \quad (\text{V}) \quad (2.5)$$

Recombination Type	Ideality Factor	Description
SRH, band to band (low level injection)	1	Recombination limited by minority carrier.
SRH, band to band (high level injection)	2	Recombination limited by both carrier types.
Auger	$2/3$	Two majority and one minority carriers required for recombination.
Depletion region (junction)	2	Two carriers limit recombination.

Table 2.1: Various Ideality Factors of  $n$

#### 2.1.4 Dark Saturation Current

The dark saturation current  $I_0$  has two potential derivations. Generally, the three parameter model, (see Baig et al. [1], MacAlpine et Brandemuehl [7], Rusirawan et Farkas [14], and others) define  $I_0$  as in Figure 2.6; where the

diode current is a function of the cell temperature and the energy bandgap in relation to several reference parameters at **STC**.

$$I_0 = I_{0,ref} \left( \frac{T_C}{T_{C,ref}} \right)^3 \exp \left( \frac{E_{G,ref}}{k_B T_{C,ref}} - \frac{E_G}{k_B T_C} \right) \quad (\text{A}) \quad (2.6)$$

On the other hand, we can derive the  $I_0$  algebraically: given the short circuit current  $I_{SC}$  and open circuit voltage ( $V_{OC}$ ), we can set the cell at open circuit, forming the derivation in Equation 2.7 and the result in Equation 2.8.

$$\begin{aligned} I_L &= 0 \\ &= I_{SC} - I_D \\ &= I_{SC} - I_0 \left[ \exp \left( \frac{V_{OC}}{V_T} \right) - 1 \right] \end{aligned} \quad (\text{A}) \quad (2.7)$$

$$I_0 = I_{SC} \left[ \exp \left( \frac{V_{OC}}{V_T} \right) - 1 \right]^{-1} \quad (\text{A}) \quad (2.8)$$

These two competing models of the dark saturation current will be explored further at the end of Chapter 2 in Section 2.4.

### 2.1.5 Short Circuit Current

Finally, for the three parameter model, we derive the dependence of  $I_{SC}$  and  $V_{OC}$  on irradiance and temperature before establishing the final derivation of Equation 2.1.

Starting with the short circuit current, it is known that there is a large positive correlation with irradiance and a small positive correlation with temperature, shown in Figures 2.3 and 2.4.

The dependence of irradiance on short circuit current can be modeled as linearly proportional to the light incident upon the solar cell over the reference irradiance. This makes intuitive sense: given half the available light (assuming the distribution of light across the spectrum is consistent), the solar cell will only be able to capture half the maximum available power. Chegaar et al. [2] proposes this relationship as Equation 2.9, where the short circuit current is a function of short circuit current constant ( $K_E$ ) and irradiance ( $G$ ) (the latter in units of  $Wm^{-2}$ ).

$$I_{SC}(G) = K_E G \quad (\text{A}) \quad (2.9)$$

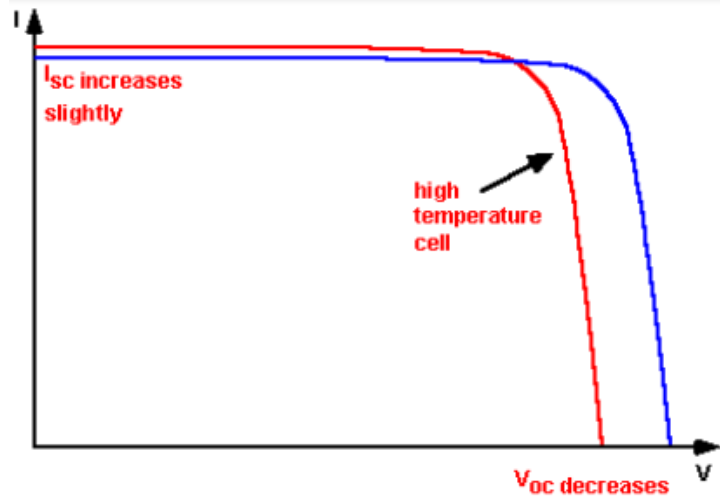


Figure 2.3: Solar Cell Temperature Dependence

Equation 2.9 can be easily reworked where the constant  $K_E$  is now based on a reference short circuit current and irradiance, preferably at STC. This forms Equation 2.10, which is the same form used by Baig et al. [1].

$$I_{SC}(G) = I_{SC,ref} \frac{G}{G_{ref}} \quad (\text{A}) \quad (2.10)$$

Hishikawa et al. [4] proposes modeling the dependence of temperature on short circuit current density using a thermal coefficient,  $\alpha$ .  $\alpha$  is empirically determined given the material composition and structure of the solar cell; for crystalline silicon solar cells, this is approximately 0.05%/K, or 0.0005. Equation 2.11 shows how given  $\alpha$ , the change in temperature affects short circuit current density and vice versa. Rearranging the equation leads to the derivation Equation 2.12. This is effectively equivalent to Rusirawan et Farkas [14], but is slightly different from MacAlpine et Brandemuehl [7] and Baig et al. [1], who take the 1 term and replaces it with a another  $I_{SC,ref}$ , shown in Equation 2.13.

$$\alpha = \frac{1}{I_{SC,ref}} \frac{\Delta I_{SC}}{\Delta T_C} = \frac{1}{I_{SC,ref}} \frac{I_{SC,ref} - I_{SC}}{T_{C,ref} - T_C} \quad (\text{unitless}) \quad (2.11)$$

$$I_{SC}(T_C) = I_{SC,ref} [1 - \alpha(T_{C,ref} - T_C)] \quad (\text{A}) \quad (2.12)$$

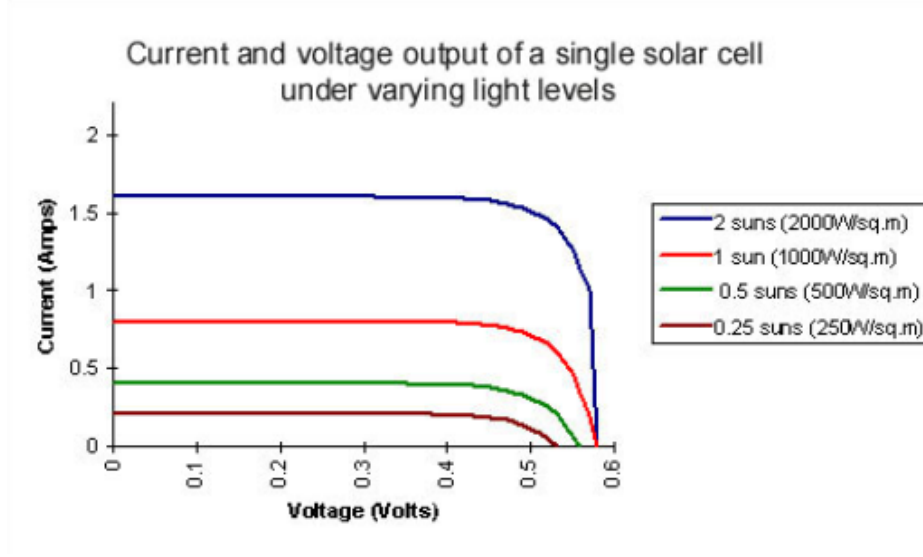


Figure 2.4: Solar Cell Irradiance Dependence

$$I_{SC}(T_C) = I_{SC,ref}[I_{SC,ref} - \alpha(T_{C,ref} - T_C)] \quad (\text{A}) \quad (2.13)$$

These two competing models of the short circuit current will also be explored further at the end of Chapter 2 in Section 2.4. For the purposes of completing this subsection, however, we will combine Equations 2.10 and 2.12 to give us Equation 2.14.

$$I_{SC}(G, T_C) = I_{SC,ref} \frac{G}{G_{ref}} [1 - \alpha(T_{C,ref} - T_C)] \quad (\text{A}) \quad (2.14)$$

### 2.1.6 Open Circuit Voltage

Likewise, the open circuit voltage is also a function of temperature and irradiance. It is known that the open circuit voltage has a medium positive correlation with irradiance and a medium negative correlation with temperature, shown back in Figures 2.3 and 2.4.

Returning to Equation 2.8, in which we defined the dark saturation current  $I_0$  as a function of the open circuit voltage  $V_{OC}$ , we can invert the equation to retrieve the  $V_{OC}$  parameter, shown in Equation 2.15.



$$V_{OC} = V_T \ln\left(\frac{I_{SC}}{I_0} + 1\right) \quad (\text{V}) \quad (2.15)$$

There are three points in this equation that can now be determined. We know from Equation 2.5 that the thermal voltage is dependent on the cell temperature  $T_C$ . We can also plug in one of the proposed models for  $I_{SC}$ . However, we cannot reuse Equation 2.8 because Equation 2.15 was derived from it! Chegaar et al. [2] simplifies the logarithmic term to form Equation 2.16.

$$V_{OC}(G, T_C) = V_{OC,ref} + V_T(T_C) \ln\left(\frac{G}{G_{ref}} + 1\right) \quad (\text{V}) \quad (2.16)$$

This term fits well with the paper's experimental data, but is not immediately clear how it models the original term. It also does not properly model temperature change. Equation 2.17 is a modified form that implements temperature dependence while retaining irradiance dependence.

$$V_{OC}(G, T_C) = V_{OC,ref}[1 - \beta(T_{C,ref} - T_C)] + \frac{nk_B(T_{C,ref} + T_C/\gamma)}{q} \ln\left(\frac{G}{G_{ref}}\right) \quad (\text{V}) \quad (2.17)$$

$$\beta = \frac{1}{V_{OC,ref}} \frac{\Delta V_{OC}}{\Delta T_C} = \frac{1}{V_{OC,ref}} \frac{V_{OC,ref} - V_{OC}}{T_{C,ref} - T_C} \quad (\text{unitless}) \quad (2.18)$$

Equation 2.17 implements two changes: a linear constant  $\beta$  that represents the open circuit voltage temperature coefficient and a modifier  $T_C/\gamma$ .  $\beta$  is likewise empirically determined given the material composition and structure of the solar cell; for silicon it known to be -0.3%/K, or -0.003.

The modifier is an experimentally determined curve fitting term, and may more appropriately model the exponential decrease of  $V_{OC}$  at low light conditions. It has an expected operable range of values between [1, 100], where smaller values correlate to a wider range of  $V_{OC}$  movement at low light conditions. This parameter, however, is not part of the three parameter cell model. Its efficacy will be explored further at the end of Chapter 2 in Section 2.4.

### 2.1.7 Model Summary

To conclude this section, we will review the components that make up the three parameter cell model, propose three items of further exploration, and propose a complete model function that incorporates in the topics discussed.

Firstly, the three parameter cell model is composed of a constant current source and a power consuming diode, representing photogeneration and recombination effects of the solar cell, respectively. These two components form three parameters that is the namesake of this section, namely the photocurrent, dark saturation current, and ideality factor.

Secondly, we explore the construction and interpretation of these three components, and along the way, examine three areas that deviate from the existing models that we would like to investigate:

- an algebraic derivation of the dark saturation current  $I_0$ ,
- an alternative interpretation of the short circuit current  $I_{SC}$  as a function of temperature,
- and a new curve fitting coefficient,  $\gamma$ , to improve open circuit voltage  $V_{OC}$  modeling at low lighting conditions.

Finally, we present the complete model function and its derivation, in Equation 2.19.

Reformat  
this  
equation

$$\begin{aligned}
I(V, G, T_C) &= I_{PV}(G, T_C) - I_D(V, G, T_C) \\
&= I_{SC}(G, T_C) - I_D(V, G, T_C) \\
&= I_{SC}(G, T_C) - I_0[\exp(\frac{V}{V_T(T_C)}) - 1] \\
&= I_{SC}(G, T_C) - I_{SC}(G, T_C)[\exp(\frac{V_{OC}(G, T_C)}{V_T(T_C)}) - 1]^{-1}[\exp(\frac{V}{V_T(T_C)}) - 1] \\
&= I_{SC}(G, T_C) - I_{SC}(G, T_C) \frac{\exp(\frac{V}{V_T(T_C)}) - 1}{\exp(\frac{V_{OC}(G, T_C)}{V_T(T_C)}) - 1} \\
&= I_{SC}(G, T_C) - I_{SC}(G, T_C) \frac{\exp(\frac{qV}{nk_B T_C}) - 1}{\exp(\frac{qV_{OC}(G, T_C)}{nk_B T_C}) - 1} \\
&= I_{SC}(G, T_C) [1 - \frac{\exp(\frac{qV}{nk_B T_C}) - 1}{\exp(\frac{qV_{OC}(G, T_C)}{nk_B T_C}) - 1}] \\
&= I_{SC,ref} \frac{G}{G_{ref}} [1 - \alpha[T_{C,ref} - T_C]] [1 - \frac{\exp(\frac{qV}{nk_B T_C}) - 1}{\exp(\frac{qV_{OC}(G, T_C)}{nk_B T_C}) - 1}] \\
&= I_{SC,ref} \frac{G}{G_{ref}} [1 - \alpha[T_{C,ref} - T_C]] \\
&\quad * [1 + \frac{1 - \exp(\frac{qV}{nk_B T_C})}{1 - \exp(\frac{q[V_{OC,ref}[1 - \beta[T_{C,ref} - T_C]] + \frac{nk_B(T_{C,ref} + T_C/\gamma)}{q} \ln(\frac{G}{G_{ref}})]}{nk_B T_C})}]
\end{aligned} \tag{A} \tag{2.19}$$

See <https://www.desmos.com/calculator/yp0rhmabkz> to play around with model. Add as figure later on compared to experimental data.

## 2.2 Five Parameter Solar Cell Model

### 2.2.1 Model Introduction

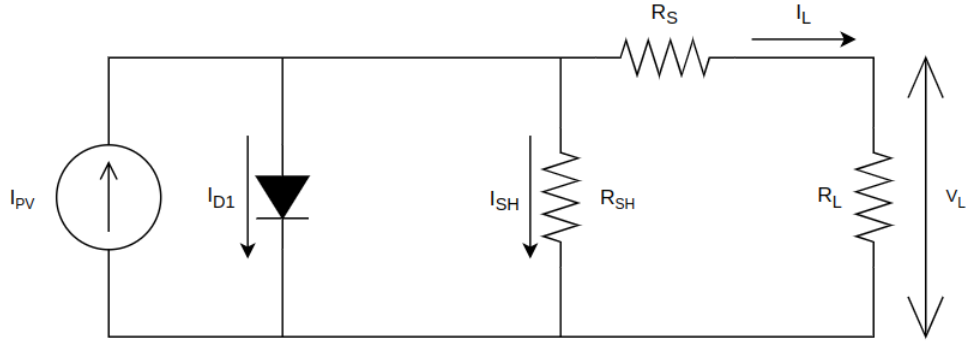


Figure 2.5: Five Parameter, or Full Single Diode Model of a Solar Cell

The most common model for solar cells is the five parameter solar cell model, shown in Figure 2.5. This is the complete form of the single diode model discussed in the previous section, Section 2.1. There are two added components/parameters: a series resistance  $R_S$  and shunt resistance  $R_{SH}$ , whose primary role is to alter the shape of the knee-bend in the I-V curve. As such, this model generally improves upon the main flaw of the three parameter solar cell model, that of overshooting the maximum power point.

In the following subsections, we discuss the two added parameters and their specific effects on the model.

### 2.2.2 Shunt Resistance

As shown in Figure 2.6 from Nelson [10], as the shunt resistance  $R_{SH}$  decreases the top of the knee-bend of the I-V curve will be forced down. At low values of shunt resistance (at the order of  $10\ \Omega$ ), the knee-bend will be pushed down so much that the curve becomes a straight line. At high values of shunt resistance, (at the order of  $100\ \Omega$ ), the curve converges to some fixed maximum bend constrained by other parameters of the model. This relationship is generally considered logarithmic.

The shunt current ( $I_{SH}$ ) is present in the simple form of the model as Equation 2.20. Assuming that the series resistance is negligible (0), we can

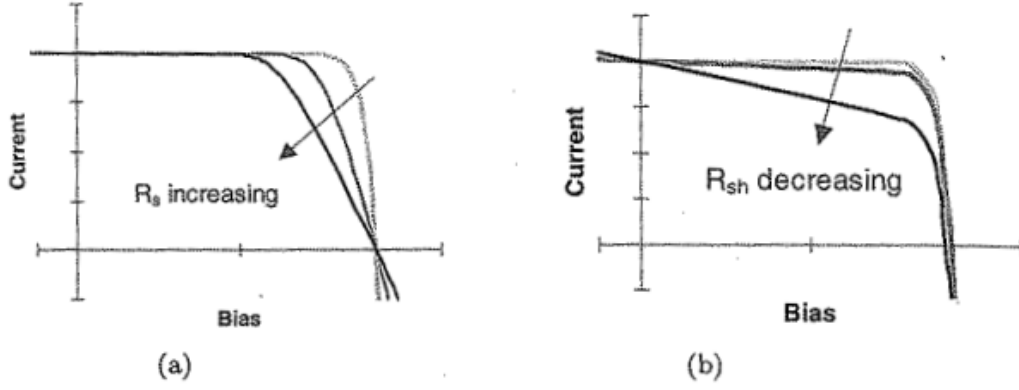


Figure 2.6: Effect of Series (a) and Shunt Resistance (b) on **I-V** Curve

determine that  $I_{SH}$  is a function of the  $R_{SH}$  and the voltage across the cell  $V$ , shown in Equation 2.21.

$$I_L = I_{PV} - I_D - I_{SH} \quad (\text{A}) \quad (2.20)$$

$$I_L = I_{PV} - I_D - \frac{V}{R_{SH}} \quad (\text{A}) \quad (2.21)$$

### 2.2.3 Series Resistance

## 2.3 Seven Parameter Solar Cell Model

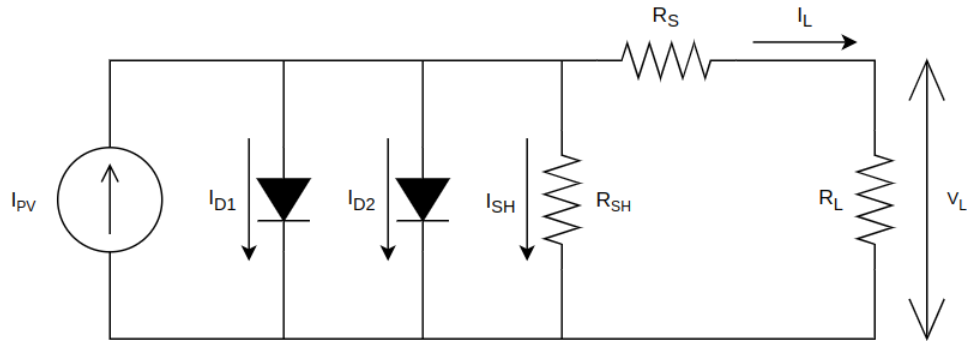
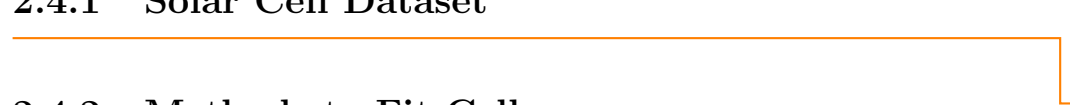


Figure 2.7: Seven Parameter, or Double Diode Model of a Solar Cell

## 2.4 Evaluation of Solar Cell Models

### 2.4.1 Solar Cell Dataset

### 2.4.2 Methods to Fit Cells



Refer  
to Ap-  
pendix  
for test-  
ing setup

## 2.5 Modeling Solar Modules



## 2.6 Evaluation of Solar Module Models

## 2.7 Modeling Solar Arrays

## 2.8 Evaluation of Solar Array Models

...

Insert  
conclu-  
sion on  
chapter  
topics  
and re-  
sults.

# Chapter 3

## Optimizing Photovoltaics

Insert intro paragraph on the focus of this chapter, as well as the a short discussion of the following sections.

Insert conclusion on chapter topics and results.

## Chapter 4

# Optimizing Photovoltaic Systems

Insert intro paragraph on the focus of this chapter, as well as the a short discussion of the following sections.

Insert sankey diagram from incident light to battery input

Insert conclusion on chapter topics and results.

## Chapter 5

## Conclusion

# Bibliography

- [1] Mirza Qutab Baig, Hassan Abbas Khan, and Syed Muhammad Ahsan. “Evaluation of solar module equivalent models under real operating conditions—A review”. In: *Journal of Renewable and Sustainable Energy* 12.1 (2020), p. 012701. DOI: [10.1063/1.5099557](https://doi.org/10.1063/1.5099557). eprint: <https://doi.org/10.1063/1.5099557>. URL: <https://doi.org/10.1063/1.5099557>.
- [2] M. Chegaar et al. “Effect of Illumination Intensity on Solar Cells Parameters”. In: *Energy Procedia* 36 (2013). TerraGreen 13 International Conference 2013 - Advancements in Renewable Energy and Clean Environment, pp. 722–729. ISSN: 1876-6102. DOI: <https://doi.org/10.1016/j.egypro.2013.07.084>. URL: <https://www.sciencedirect.com/science/article/pii/S1876610213011703>.
- [3] R.N. Hall. “Silicon photovoltaic cells”. In: *Solid-State Electronics* 24.7 (1981), pp. 595–616. ISSN: 0038-1101. DOI: [https://doi.org/10.1016/0038-1101\(81\)90188-X](https://doi.org/10.1016/0038-1101(81)90188-X). URL: <https://www.sciencedirect.com/science/article/pii/003811018190188X>.
- [4] Yoshihiro Hishikawa et al. “Temperature dependence of the short circuit current and spectral responsivity of various kinds of crystalline silicon photovoltaic devices”. In: *Japanese Journal of Applied Physics* 57.8S3 (July 2018), 08RG17. DOI: [10.7567/JJAP.57.08RG17](https://doi.org/10.7567/JJAP.57.08RG17). URL: <https://dx.doi.org/10.7567/JJAP.57.08RG17>.
- [5] *Ideality factor*. PVEducation. URL: <https://www.pveducation.org/pvcdrom/solar-cell-operation/ideality-factor#:~:text=The%20ideality%20factor%20of%20a,certain%20assumptions%20about%20the%20cell..>

- [6] Amit Jain and Avinashi Kapoor. “A new method to determine the diode ideality factor of real solar cell using Lambert W-function”. In: *Solar Energy Materials and Solar Cells* 85.3 (2005), pp. 391–396. ISSN: 0927-0248. DOI: <https://doi.org/10.1016/j.solmat.2004.05.022>. URL: <https://www.sciencedirect.com/science/article/pii/S0927024804002442>.
- [7] Sara M. MacAlpine and Michael J. Brandemuehl. “Photovoltaic module model accuracy at varying light levels and its effect on predicted annual energy output”. In: *2011 37th IEEE Photovoltaic Specialists Conference*. 2011, pp. 002894–002899. DOI: [10.1109/PVSC.2011.6186551](https://doi.org/10.1109/PVSC.2011.6186551).
- [8] Gaetan Masson et al. *Snapshot of Global PV Markets 2022 Task 1 Strategic PV Analysis and Outreach PVPS*. Apr. 2022. ISBN: 978-3-907281-31-4.
- [9] Gaetan Masson et al. *Trends in Photovoltaic Applications 2022*. Oct. 2022. ISBN: 978-3-907281-35-2.
- [10] Jenny Nelson. “Introduction”. In: *The physics of Solar Cells*. Imperial College Press, 2013, p. 14.
- [11] *Net Zero by 2050*. Paris: IEA Photovoltaic Power Systems Programme, 2021.
- [12] Santiago Pindado, Javier Cubas, and Carlos Manuel. “Explicit Expressions for Solar Panel Equivalent Circuit Parameters Based on Analytical Formulation and the Lambert W-Function”. In: *Energies* 7 (June 2014), pp. 4098–4115. DOI: [10.3390/en7074098](https://doi.org/10.3390/en7074098).
- [13] United Nations Environment Programme. *Paris Agreement*. 12/12/2015. URL: <https://wedocs.unep.org/20.500.11822/20830>.
- [14] Dani Rusirawan and István Farkas. “Identification of Model Parameters of the Photovoltaic Solar Cells”. In: *Energy Procedia* 57 (2014). 2013 ISES Solar World Congress, pp. 39–46. ISSN: 1876-6102. DOI: <https://doi.org/10.1016/j.egypro.2014.10.006>. URL: <https://www.sciencedirect.com/science/article/pii/S1876610214013733>.
- [15] Brady Tyra et al. *Electric Power Monthly*. U.S. Energy Information Administration, Oct. 2022. URL: <https://www.eia.gov/electricity/monthly/archive/october2022.pdf>.



# Appendices

# Appendix A

## Acronyms and Abbreviations

<b>BPS</b>	battery protection system
<b>EIA</b>	U.S. Energy Information Administration
<b>GW</b>	Gigawatts
<b>IEA</b>	International Energy Association
<b>I-V</b>	current-voltage
<b>LHRs</b>	Longhorn Racing Solar
<b>MPPT</b>	maximum power point tracking
<b>PV</b>	photovoltaic
<b>P-V</b>	power-voltage
<b>STC</b>	standard test conditions
<b>UN</b>	United Nations

# Appendix B

## Mathematical Nomenclature

$A$  area

$b_S(E)$  spectral photon flux density

$E$  energy

$G$  irradiance

$I_L$  load current

$I_D$  dark current, or diode current

$I_{PV}$  photocurrent, or light generated current

$I_S$  series current

$I_{SC}$  short circuit current

$I_{SH}$  shunt current

$I_0$  dark saturation current, or reverse saturation current

$K_B$  Boltzmann constant

$K_E$  short circuit current constant

$n$  ideality factor

$QE(E)$  quantum efficiency

$q$  electric charge constant

$R_L$  load resistance

$R_S$  series resistance

$R_{SH}$  shunt resistance

$T_C$  cell temperature

$V$  load voltage

$V_T$  thermal voltage

$V_{OC}$  open circuit voltage

# TODOS

■ The second area of development may be more generalized then this.	6
■ Insert intro paragraph on the focus of this chapter, as well as the a short discussion of the following sections. . . . .	8
■ Reformat this equation . . . . .	17
■ See <a href="https://www.desmos.com/calculator/yp0rhmabkz">https://www.desmos.com/calculator/yp0rhmabkz</a> to play around with model. Add as figure later on compared to experimental data.	18
■ Refer to Appendix for testing setup . . . . .	22
■ Insert conclusion on chapter topics and results. . . . .	26
■ Insert intro paragraph on the focus of this chapter, as well as the a short discussion of the following sections. . . . .	27
■ Insert conclusion on chapter topics and results. . . . .	27
■ Insert intro paragraph on the focus of this chapter, as well as the a short discussion of the following sections. . . . .	28
■ Insert sankey diagram from incident light to battery input . . . . .	28
■ Insert conclusion on chapter topics and results. . . . .	28